DOI 10.1007/s10778-024-01269-7
International Applied Mechanics, Vol. 60, No. 2, March, 2024

DEVELOPMENT OF PLASTIC ZONE NEAR TIP OF INTERFACIAL CRACK WITH CONTACTING FACES

A. O. Kaminsky[1*] and M. V. Dudyk[2]**

The parameters of a narrow small-scale plastic zone in an elastoplastic piece-wise homogeneous body undergoing a shear near the tip of an interfacial crack are calculated under plane strain conditions using the Wiener-Hopf method. Crack faces are in contact with friction. The plastic zone issuing out of the crack tip at an angle to a plane interface between media is modeled as the straight line of a displacement discontinuity involving two sections. Both tangential and normal displacements undergo the discontinuity at the section adjacent to the crack tip that models material destruction area. At the other section, only the tangential displacement experiences the discontinuity. The angle between the plastic zone and interface between the media is defined from the condition that the rate of energy dissipation in the zone is maximal. The sizes of the entire plastic zone, destruction zone and shear opening displacement of the crack in its tip are determined. It is studied how the friction of the crack faces, load, and the mechanical characteristics of the material influence on the parameters of the plastic zone and stress-strain state in the vicinity of the crack tip.

Keyword: interfacial crack, contact of the crack faces, plastic zone, destruction zone

Introduction. The stress concentration near a crack tip in quasi-brittle and plastic materials causes an origin of plastic zone in the body, which strongly influences on its stress-strain state (SSS). If the crack lies at interface between dissimilar materials, appear additional factors which should be allowed for in the SSS calculations. Moreover, if a piece-wise homogeneous body with an interfacial crack is acted upon by shear load, the crack faces near one of the crack tips are in contact which covers the area whose sizes are close to the crack length. This phenomenon is described within the framework of the Comninou contact model of an interfacial crack [7, 8] developed in [1, 4, 9, 14, 15, 21, 28, 33]. At that, the contact of the crack faces does not eliminate stress concentration in the tip vicinity and formation of the plastic zone.

To calculate the parameters of the plastic zone near the tip of an interfacial crack is difficult mathematical problem which is solved mainly by numerical methods. So, Shih and Asaro, using the finite element method numerically have calculated an elastoplastic field under small-scale yielding near the tip of open crack at interface between elastoplastic and linear elastic materials undergoing the action of mixed external loading [35]. It is revealed that the plastic zone elongates mainly with the increasing load in the direction of the resulting vector of external forces. Also it is established that the contact zone formed need not be adjacent to the crack tip. Besides, the finite element method is involved by Aravas and Sharma in solving the problem on the plastic zone near the crack tip arranged at interface between an elastoplastic material and a rigid pillow. It is assumed that the crack faces contact without friction, while the external tensile load is applied under the plane strain state [2] and the plane stress state [3]. Furthermore, the deformation of the nonlinearly reinforced elastoplastic material is described by the Ramberg–Osgood equation of the deformation plasticity theory. The results obtained have demonstrated that the stresses differ from those found in elastic solving with the Comninou model. It is established that the small-scale plastic zone adjoins to the contacting section of

[1]Timoshenko Institute of Mechanics of the National Academy of Sciences of Ukraine, 3 Nesterova St., 03057, Kyiv, Ukraine; *e-mail: dfm11@ukr.net. [2]Uman Pavlo Tychyna State Pedagogical University, 2 Sadova St., 20300, Uman, Ukraine; **e-mail: dudik_m@hotmail.com. Translated from Prykladna Mekhanika, Vol. 60, No. 2, pp. 32–47, March–April 2024. Original article submitted August 03, 2023.

faces and elongates along the interface. In [30], Nakatani et al. using the continual theory with slip lines and the discrete dislocation plasticity theory have studied numerically, under the plane strain state, the small-scale yielding near the tip of a stationary crack at interface between a plastic monocrystal and rigid material. It is revealed that in this case two slip bands are formed, which under the two-axial tension propagate beginning from the crack tip both at an acute and a blunt angle to the interface.

The experimental investigations of fracture processes in solids have shown that the plastic zone directly near a crack tip includes the small area of destructed material with a very high level of strains [17, 24, 25]. This factor should be allowed for also in studying the SSS near the tip of the interfacial crack. One way to solve the problem is adaptation to its purposes of basic regulations of the complex model of the interfacial crack developed for studying a prefracture zone in a less crack-resistant composite material [19, 23]. Here, the prefracture zone is modeled as a line of displacement discontinuity that consists of two sections. In the first section, the prefracture zone is modeled as a segment with discontinuity of normal displacement. To model the destruction zone, it is necessary to include in the section of the segment adjacent to the crack tip the discontinuity of the tangential displacement.

The purpose of the present work is to develop the model of a plastic zone at the end of the interfacial crack with contacting faces at the initial stage of propagation of this zone when its length is considerably lesser than that of the contact area. By analogy with the complex model of the interfacial crack [19, 23], it is assumed that the zone develops in two stages. At the first stage, once the body has been loaded and the contact zone forms, narrow plastic zone origins in softer composite material. Since its formation does not exclude stress concentration near the crack tip, this leads to formation at the other stage of propagation of an area with increased strains known as the destruction area. To determine the parameters of the area under the plane strain condition, the Dugdale model [11] and the Leonov–Panasyuk model [27] will be used and the two following problems will be solved.

In the first problem, we calculate, using the Wiener-Hopf method, the parameters of the initial plastic zone. It will be modeled as the lateral line of discontinuity of the tangential displacement issuing out from the tip of the interfacial crack whose faces interact in accordance with the dry friction law. We will allow for loading conditions and body configuration in terms of the stress intensity factor at the crack tip which is assumed to be known. To define orientation of the plastic zone, we will use the condition by which the energy dissipation rate in the zone is maximal [5]. The results obtained will be involved in solving the second problem on the destruction area which is modeled by the additional discontinuity of the normal displacement in the section of the plastic zone adjacent to the crack tip.

The results of numerical calculations of the parameters of plastic zone with the intrinsic destruction zone in the partial case of a piecewise homogeneous plane with the interfacial crack of finite length loaded at infinity by homogeneous shear load will be presented in conclusion.

1. Determination of the Parameters of an Initial Plastic Zone. Consider a problem on the initial stage of development of a plastic zone from the crack tip, which is arranged in a piece-wise homogeneous body at a plane interface between two dissimilar isotropic elastoplastic materials acted upon by shear load. Shear moduli and Poisson's ratios of the materials are G_1, G_2 and ν_1, ν_2, respectively. At this stage a narrow band-like plastic zone origins near the tip in the material with elastic constants G_1 and ν_1. It is assumed that this material is more plastic, while both materials demonstrate linear elasticity everywhere but with the exception of the plasticity zone.

We will model the plastic zone by a straight line of discontinuity of a tangential displacement [34]. The line issues out from the crack tip at an angle α to the interface between materials. In accordance with the Tresca-Saint-Venant plastic criterion, the shear stress takes the value of the yield point of the first material τ_{1s}.

It should be noted that the Comninou model assumes presence near the opposite crack tips of different in sizes both large and very small areas with contacting faces. For the sake of definiteness, we will adopt that $G_1 < G_2$, while the shear load τ_{xy} acts in the direction as in Fig. 1. Then, according to [1, 7, 9, 14, 33], the length s of the contact zone near the crack tip O will be commensurable with the crack length L and considerably larger (at a sufficient level of a load) than the length l of the plastic zone at the initial stage of the development studied. In the case of an oppositely directed shear load, the sizes of the contact zone near the tip O will be extremely small. At that, we will arrive at the problem on the small-scale plastic zone near the tip of an open interfacial crack solved in [18].

Note that determination of the parameters of the plastic zone can be restricted by studying its SSS only in vicinity. Then, we will consider the problem for a piece-wise homogeneous isotropic plane with a semi-infinite interface crack, whose contacting faces interact in accordance with the dry friction law, as the solution of the respective boundary-value elasticity

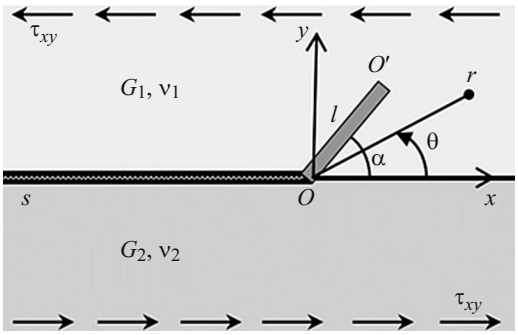


Fig. 1

problem. The plane includes also the finite-length line of the tangential displacement discontinuity, which issues out from the crack tip into the first material at an angle of α to the interface between the materials. Involving the Prandtl method of joining asymptotic expansions [31], we formulate the condition at infinity as demand to join at the distances $l << r << s$ of the searched problem solution, shown in Fig. 1, with the solution of the similar elasticity problem on the interfacial crack with a contact zone near its tip when the lateral discontinuity line is absent. Such solution is presented in [1, 7, 9, 33]. As a result, we arrive at a static elasticity problem with following boundary conditions (Fig. 1):

$$\theta = 0, \quad \langle \sigma_\theta \rangle = \langle \tau_{r\theta} \rangle = 0, \quad \langle u_\theta \rangle = \langle u_r \rangle = 0,$$

$$\theta = \alpha, \quad \langle \sigma_\theta \rangle = \langle \tau_{r\theta} \rangle = 0, \quad \langle u_\theta \rangle = 0,$$

$$\theta = \pm\pi, \quad \langle \sigma_\theta \rangle = \langle \tau_{r\theta} \rangle = 0, \quad \langle u_\theta \rangle = 0, \quad \tau_{r\theta} = -\mu\sigma_\theta, \tag{1}$$

$$\theta = \alpha, \quad r < l, \quad \tau_{r\theta} = \tau_1, \quad \theta = \alpha, \quad r > l, \quad \langle u_r \rangle = 0, \tag{2}$$

$$\theta = \alpha, \quad r \to \infty, \quad \tau_{r\theta} = k_{II} F(\alpha) r^{\lambda} + o(1/r), \tag{3}$$

$$F(\alpha) = \frac{(2\pi)^{\lambda}}{2} \{[2 + \lambda(1+\beta)]\cos(2+\lambda)\alpha - \lambda(1+\beta)\cos\lambda\alpha\},$$

$$\beta = \frac{(1+e\kappa_2) - (e+\kappa_1)}{(1+e\kappa_2) + (e+\kappa_1)}, \quad e = \frac{G_1}{G_2} \quad (G_1 < G_2), \quad \kappa_{1(2)} = 3 - 4\nu_{1(2)},$$

where $\langle f \rangle$ is the discontinuity in the value of f; $\tau_1 = \tau_{1s}\mathrm{sgn}(k_{II} F(\alpha))$, μ is the coefficient of friction between the crack faces; β is the so called second Dundurs parameter [12], which represents the measure of difference in elastic properties of joined materials $|\beta| \le 0.5$, λ is the real root of an equation $\cot\lambda\pi + \mu\beta = 0$ at the interval $(-1, 0)$, which indicates the stress singularity near the tip of a crack with contacting faces. If the upper material shifts in the direction $\theta = \pi$ (Fig. 1), the friction coefficient becomes negative. The stress intensity factor k_{II} at the end of the interfacial crack depends on configuration of the body under consideration and of the applied load given by the condition. To provide a compressive stress on the crack faces in the contacting zone $\theta = \pi$, $\sigma_\theta < 0$, the factor k_{II} must meet the condition $\beta k_{II} > 0$ [26].

In accordance with the general regulations, which refer to the behavior of the stresses near angular points in elastic bodies [6], at the end O' of the discontinuity line the asymptotic is realized. It represents the asymptotic solution of a homogeneous elasticity problem for a plane with a semi-infinite line of discontinuity of the tangential displacement. In particular, the following asymptotics are valid:

$$\theta = \alpha, \quad r \to l + 0, \quad \tau_{r\theta} \sim \frac{k}{\sqrt{2\pi(r-l)}},$$

$$\theta = \alpha, \quad r \to l - 0, \quad \tau_{r\theta} \sim -\frac{2(1-\nu_1)}{G_1} \frac{k}{\sqrt{2\pi(l-r)}}, \tag{4}$$

where k is the stress intensity factor at the end of the discontinuity line. Its value is defined during problem solving.

We will search for the solution of the boundary-value problem (1)–(4) as the sum of solutions of two following problems. The first one differs from it in that in (2) instead of the first condition, we believe that

$$\theta = \alpha, \quad r < l, \quad \tau_{r\theta} = \tau_1 - k_{II} F(\alpha) r^{\lambda}, \tag{5}$$

while at infinity stresses decay as o(1/r). The second problem is analogical to that one without the discontinuity line, whose solution is known [1, 7, 9, 33]. Because of this, it is sufficient to solve the first problem.

Having applied to the equilibrium equations the condition of strains consistency, Hooke's law, the boundary conditions (1), the Mellin integral transformation [36], with allowance for the second condition (2) and condition (5) we arrive at the Wiener-Hopf functional equation of the first problem on the interval $-\delta_1 < \mathrm{Re}\, p < \delta_2$ (δ_1, δ_2 are the sufficiently small positive numbers):

$$\Phi^+(p) + \frac{\tau_1}{p+1} + \frac{\tau_2}{p+\lambda+1} = \cot p\pi \cdot G(p)\Phi^-(p), \tag{6}$$

$$\Phi^+(p) = \int_1^{\infty} \tau_{r\theta}(\rho l, \alpha)\rho^p d\rho, \quad \Phi^-(p) = \frac{G_1}{2(1-\nu_1)} \int_0^1 \left\langle \frac{\partial u_r}{\partial r} \right\rangle \Bigg|_{\substack{r=\rho l \\ \theta=\alpha}} \rho^p d\rho,$$

$$\tau_2 = -k_{II} F(\alpha) l^{\lambda}, \quad G(p) = \frac{D_1(p)}{\cos^2 p\pi D_0(p)},$$

$$D_0(p) = 2(e+\kappa_1)(1+e\kappa_2)[(e+\kappa_1)+(1+e\kappa_2)]\{1-\mu\beta\tan p\pi\},$$

$$D_1(p) = D_{10}(p) + \mu D_{11}(p),$$

$$D_{10}(p) = (1+\kappa_1)^2\left[(1+\kappa_1)\delta_1(p) + e(1+\kappa_2)\delta_2(p) + (1-e)\delta_3(p)\right]$$

$$+ (1+\kappa_1)\left[(1-e)^2\delta_4(p) + e^2(1+\kappa_2)^2\delta_5(p)\right] + e(1+\kappa_2)(1-e)\left[(1+e\kappa_2)\delta_6(p) + (1+\kappa_1)\delta_7(p)\right],$$

$$\delta_1(p) = \sin^2\alpha - \sin^2 p(\pi-\alpha),$$

$$\delta_2(p) = p\sin 2\alpha \sin 2p\alpha + 2(\sin^2\alpha\cos 2p\alpha + \sin^2 p\alpha - \sin^2 p\pi),$$

$$\delta_3(p) = \sin 2p\alpha\left[p\sin 2\alpha - \sin 2p(\pi-\alpha)\right] - 4\sin^2 p\alpha\delta_1(p),$$

$$\delta_4(p) = 4\left[\sin^2\alpha\sin^2 p\alpha + \sin p\alpha \sin p(\pi-\alpha)\cos p\pi - p^2\sin^2\alpha\cos^2 p(\pi-\alpha)\right]$$

$$- p\sin 2\alpha\left[\sin 2p\alpha - \sin 2p(\pi-\alpha)\right],$$

$$\delta_5(p) = \sin^2\alpha(1-4p^2\sin^2 p\alpha) + p\sin 2\alpha\sin 2p\alpha - \sin p(\pi-\alpha)\left[\sin p(\pi+\alpha) + 2\cos p\pi\sin p\alpha\right],$$

$$\delta_6(p) = 2\cos p\pi\left[2\sin p(\pi-\alpha)\sin p\alpha + p\sin 2\alpha\sin p(\pi-2\alpha) - 2p^2\sin^2\alpha\cos p(\pi-2\alpha)\right],$$

$$\delta_7(p) = 4\sin^2\alpha\left[(1-p^2)\sin^2 p\alpha - p^2\cos^2 p(\pi-\alpha)\right] + p\sin 2\alpha\sin 2p(\pi-\alpha),$$

$$D_{11}(p) = -(1+\kappa_1)\overline{D}_{11}(p) - 2(1-e)\widetilde{D}_{11}(p),$$

$$\overline{D}_{11}(p) = (1+\kappa_1)^2\overline{\delta}_1 + e^2(1+\kappa_2)^2\overline{\delta}_2 + 4(1-e)^2\sin p\pi\overline{\delta}_3$$

$$+ (1+\kappa_1)e(1+\kappa_2)2\overline{\delta}_4 + (1-e)(1+\kappa_1)2\overline{\delta}_5 + e(1+\kappa_2)(1-e)\overline{\delta}_6,$$

$$\widetilde{D}_{11}(p)=(1+\kappa_1)^2\,\widetilde{\delta}_1+\left[e^2(1+\kappa_2)^2+2(1-e)^2+3e(1+\kappa_2)(1-e)\right]\sin p\pi\widetilde{\delta}_2+(1+\kappa_1)\left[e(1+\kappa_2)\widetilde{\delta}_3+2(1-e)\widetilde{\delta}_4\right],$$

$$\overline{\delta}_1(p)=0.5\left[\sin 2\alpha-\sin 2p(\pi-\alpha)\right],$$

$$\overline{\delta}_2(p)=2p^2\sin^2\alpha\sin 2p\alpha+(1-2p\cos 2p\alpha)\sin\alpha\cos\alpha$$

$$+\sin p(\pi-\alpha)\left[\cos p(\pi+\alpha)-2\sin p\pi\sin p\alpha\right],$$

$$\overline{\delta}_3(p)=p\sin\alpha\left[2p\sin\alpha\sin p(\pi-\alpha)\sin p\alpha-\cos p\alpha\sin\left(p(\pi-\alpha)-\alpha\right)\right]$$

$$+\sin p\alpha\left[\sin\alpha\cos\left(p(\pi-\alpha)+\alpha\right)-\sin p(\pi-\alpha)\right],$$

$$\overline{\delta}_4(p)=-p\sin\alpha(\cos\alpha+\sin\alpha\sin 2p\alpha)+\sin\alpha\cos\alpha\cos 2p\alpha+2\sin p\alpha\sin p\pi\sin p(\pi-\alpha),$$

$$\overline{\delta}_5(p)=-p\sin\alpha\left[\sin\alpha\sin 2p\alpha+\sin p(\pi-\alpha)\sin\left(p(\pi-\alpha)+\alpha\right)\right]-\sin 2\alpha\sin^2 p\alpha$$

$$+\sin p(\pi-\alpha)\left[2\sin p\alpha\sin p\pi+\sin\alpha\sin\left(p(\pi-\alpha)+\alpha\right)\right],$$

$$\overline{\delta}_6(p)=2p^2\sin^2\alpha\sin p\alpha\left[2\cos p\alpha-\cos p(2\pi-\alpha)\right]$$

$$+p\sin\alpha\left[2\cos\alpha\left(\sin^2 p\alpha-\sin^2 p(\pi-\alpha)\right)-\sin p(\pi+\alpha)\sin\left(p(\pi-\alpha)-\alpha\right)\right]$$

$$+\sin\alpha\left[\cos\alpha-\cos\left(p(\pi-\alpha)+\alpha\right)\right]-4\sin p\alpha\sin p\pi\sin p(\pi-\alpha),$$

$$\widetilde{\delta}_1(p)=\cos\left(p(\pi-\alpha)+\alpha\right)\left[\cos\alpha\sin p(\pi-\alpha)-p\sin\alpha\cos p(\pi-\alpha)\right],$$

$$\widetilde{\delta}_2(p)=p\sin 2\alpha\sin p(\pi-2\alpha)-2p^2\sin^2\alpha\cos p(\pi-2\alpha)+2\sin p\alpha\sin p(\pi-\alpha),$$

$$\widetilde{\delta}_3(p)=+p\sin\alpha\left[2\cos\alpha\sin^2 p\alpha-\cos p(\pi+\alpha)\cos\left(p(\pi-\alpha)-\alpha\right)\right]+p^2\sin^2\alpha$$

$$\times(\sin 2p\alpha+\sin 2p\pi)+\sin p(\pi-\alpha)\left[\cos\alpha\cos\left(p(\pi+\alpha)+\alpha\right)-2\sin p\pi\sin p\alpha\right],$$

$$\widetilde{\delta}_4(p)=0.5p^2\sin^2\alpha(\sin 2p\alpha+\sin 2p\pi)+p\sin\alpha\left[\cos p\pi\sin p(\pi-\alpha)\sin\left(p-1\right)\alpha+2\cos\alpha\sin^2 p\alpha\right]$$

$$-\sin p(\pi-\alpha)\sin p\alpha\left[\sin p\pi+\cos\alpha\sin(p\pi+\alpha)\right].$$

The function $G(it)\,(-\infty<t<\infty)$ for $\mu\cot\alpha<1$ has paired positive real and unpaired imaginary sections, which at $t\to\pm\infty$ go to 1 and 0, respectively. Because of this, the index of the function $G(p)$ along the axis is equal to 0, while the factorization is valid according to formula [13]

$$G(p)=\frac{G^+(p)}{G^-(p)}\quad(\mathrm{Re}\,p=0),$$

$$\exp\left[\frac{1}{2\pi i}\int\limits_{-i\infty}^{i\infty}\frac{\ln G(z)}{z-p}\,dz\right]=\begin{cases}G^+(p), & \mathrm{Re}\,p<0,\\ G^-(p), & \mathrm{Re}\,p>0.\end{cases}$$

Besides, the following factorization holds:

$$p\cot p\pi=K^+(p)K^-(p),\qquad K^\pm(p)=\frac{\Gamma(1\mp p)}{\Gamma(1/2\mp p)},$$

where $\Gamma(z)$ is the Euler gamma-function. In this case equation (6) becomes

$$\frac{\Phi^+(p)}{K^+(p)G^+(p)}+\frac{\tau_1}{p+1}\left[\frac{1}{K^+(p)G^+(p)}-\frac{1}{K^+(-1)G^+(-1)}\right]$$

$$+\frac{\tau_2}{p+\lambda+1}\left[\frac{1}{K^+(p)G^+(p)}-\frac{1}{K^+(-\lambda-1)G^+(-\lambda-1)}\right]$$

$$=\frac{\Phi^-(p)K^-(p)}{pG^-(p)}-\frac{\tau_1}{(p+1)K^+(-1)G^+(-1)}-\frac{\tau_2}{(p+\lambda+1)K^+(-\lambda-1)G^+(-\lambda-1)} \quad (\mathrm{Re}\, p=0). \tag{7}$$

The function appearing in the left side of (7) is analytical in the half-plane Re $p<0$, while the function appearing in the right side is analytical in the plane Re $p>0$. Then, in accordance with the principle of analytical continuation, a unified function analytical over the whole plane of the complex variable p equal to the left and right sides of equality (7) must be presented in the respective half-planes. To determine the function, applying the Abel-type theorem [32] to asymptotics (4), we obtain:

$$\Phi^+(p)\sim\frac{k}{\sqrt{-2pl}} \quad (p\to\infty, \mathrm{Re}\, p<0),$$

$$\Phi^-(p)\sim-\frac{k}{\sqrt{2pl}} \quad (p\to\infty,\ \mathrm{Re}\, p>0). \tag{8}$$

With (8) as well as the asymptotics $G^+(p)\to 1, K^+(p)\sim\sqrt{-p}\,(p\to\infty, \mathrm{Re}\, p<0), G^-(p)\to 1, K^-(p)\sim\sqrt{p}\,(p\to\infty,$ Re $p>0)$, we reveal that the left and right sides of equality (7) at $p\to\infty$ go to zero. Then, by the Liouville theorem, the unified analytical function becomes identically equal to zero. Whence we arrive at the exact analytical solution of equation (6):

$$\Phi^+(p)=-K^+(p)G^+(p)\left\{\frac{\tau_1}{p+1}\left[\frac{1}{K^+(p)G^+(p)}-\frac{1}{K^+(-1)G^+(-1)}\right]\right.$$

$$\left.+\frac{\tau_2}{p+\lambda+1}\left[\frac{1}{K^+(p)G^+(p)}-\frac{1}{K^+(-\lambda-1)G^+(-\lambda-1)}\right]\right\} \quad (\mathrm{Re}\, p<0),$$

$$\Phi^-(p)=\frac{pG^-(p)}{K^-(p)}\left[\frac{\tau_1}{(p+1)K^+(-1)G^+(-1)}+\frac{\tau_2}{(p+\lambda+1)K^+(-\lambda-1)G^+(-\lambda-1)}\right] \quad (\mathrm{Re}\, p>0). \tag{9}$$

With (9), we find the asymptotic

$$\Phi^+(p)\sim\frac{-1}{\sqrt{-p}}\left[\frac{\tau_1}{K^+(-1)G^+(-1)}+\frac{\tau_2}{K^+(-\lambda-1)G^+(-\lambda-1)}\right] \quad (p\to\infty).$$

Comparing it with (8), we determine the stress intensity factor at the end of the discontinuity line:

$$k=-\sqrt{2l}\left[\frac{\tau_1}{K^+(-1)G^+(-1)}+\frac{\tau_2}{K^+(-\lambda-1)G^+(-\lambda-1)}\right]. \tag{10}$$

Equating the right side of expression (10) to zero and allowing for the fact that the value of stresses at the end of the plastic zone is finite, we arrive at the expression for its length

$$l=\left(\frac{2k_{II}F(\alpha)J(0)}{\sqrt{\pi}\tau_1K^+(-\lambda-1)J(\lambda)}\right)^{-1/\lambda}, \tag{11}$$

$$J(x)=\exp\left[\frac{1}{\pi}\int_0^{\infty}\frac{(x+1)\ln|G(it)|+t\cdot\arg G(it)}{t^2+(x+1)^2}\,dt\right].$$

To determine the orientation of the initial plastic zone, we will employ the criterion of maximal energy dissipation rate in the zone. To this end, we define the value of the energy dissipation, which within the framework of the chosen model in accordance with [5] and formula for transform $\Phi^-(1)$ in (6) is written as

$$W=\tau_1\int_0^{l}\langle u_r(r,\alpha)\rangle\,dr=-\frac{2(1-\nu_1)}{G_1}\,l^2\tau_1\,\Phi^-(1).$$

Substituting solution (9) of the Wiener–Hopf equation of the problem in this expression, with (11), we get the following formula for the rate of the energy dissipation in the zone:

$$\frac{dW}{dt}=\frac{\pi(1-\nu_1)\tau_{1s}^2}{2(2+\lambda)G_1}\left(\frac{|k_{II}(t)|}{\tau_{1s}}\right)^{-2/\lambda}\frac{1}{k_{II}(t)}\frac{dk_{II}(t)}{dt}\,w(\alpha), \tag{12}$$

$$w(\alpha)=\frac{J_1(0)}{J(0)}\left(\frac{2|F(\alpha)|J(0)}{\sqrt{\pi}K^+(-\lambda-1)J(\lambda)}\right)^{-2/\lambda},$$

$$J_1(x)=\exp\left[\frac{-1}{\pi}\int_0^{\infty}\frac{(x+1)\ln|G(it)|-t\cdot\arg G(it)}{t^2+(x+1)^2}\,dt\right].$$

Having assumed that k_{II} is either a positive increasing or negative decreasing time function, we arrive at the condition $w(\alpha)\to\max$, which will be used in calculating the angle of inclination of the plastic zone.

According to (11), the length of the plastic zone increases nonlinearly with the increase of the external load, which enters linearly in the stress intensity factor k_{II}. Besides, the greater is length of the plastic zone, the less is the yield point τ_{1s} of material in which the plastic zone develops.

Using (9) and the reverse Mellin transformation, we define the stress field near the crack tip which has changed once the plastic zone has been formed. In particular, the normal stress at the discontinuation line which is in need to determine the destruction area is:

$$\sigma_\theta(r,\alpha)=\tau_1\left[\frac{N(-1)}{D_1(-1)}+\sum_i\frac{N(-1-\lambda_i)}{D_1'(-1-\lambda_i)}\frac{K^+(-1-\lambda_i)}{K^+(-1)}\frac{J(\lambda_i)}{J(0)}\frac{\lambda}{\lambda_i(\lambda_i-\lambda)}\left(\frac{r}{l}\right)^{\lambda_i}\right]\quad(r\ll l), \tag{13}$$

$$D_1'(p)=dD_1(p)/dp,\qquad N(p)=N_1(p)+\mu N_2(p),$$

$$N_1(p)=(1+\kappa_1)\left[(1+\kappa_1)^2u_{11}+e^2(1+\kappa_2)^2u_{12}-(1+\kappa_1)e(1+\kappa_2)u_{13}\right]$$

$$+(1-e)\left[(1+\kappa_1)^2v_{11}+2e(1+\kappa_2)(1+e\kappa_2)v_{12}+(1+\kappa_1)\left(e(1+\kappa_2)v_{13}+(1-e)v_{14}\right)\right],$$

$$u_{11}(p)=0.5\left[\sin 2\alpha-\sin 2p(\pi-\alpha)\right],$$

$$u_{12}(p)=2p(p-1)\sin^2\alpha\sin 2p\alpha-p\sin 2\alpha+0.5\left[\sin 2\alpha+\sin 2p(\pi-\alpha)\right],$$

$$u_{13}(p)=(p-1)\sin 2\alpha\cos 2p\alpha,$$

$$v_{11}(p)=2(p-1)\sin 2\alpha\sin^2 p\alpha-p\sin 2\alpha+\sin 2p(\pi-\alpha),$$

$$v_{12}(p) = 2p(p-1)\sin^2\alpha \sin p(\pi-2\alpha)\cos p\pi,$$

$$v_{13}(p) = 4(p-1)\left[p\sin^2\alpha \sin p\pi\cos p(\pi-2\alpha) - \sin 2\alpha \sin^2 p\alpha\right] + v_{11}(p),$$

$$v_{14}(p) = 2(p-1)\left[p\sin^2\alpha \sin 2p(\pi-\alpha) - \sin 2\alpha \sin^2 p\alpha\right],$$

$$N_2(p) = (1+\kappa_1)\left[(1+\kappa_1)^2 u_{21} + e^2(1+\kappa_2)^2 u_{22} - 2(1+\kappa_1)e(1+\kappa_2)u_{23}\right]$$

$$-4(1-e)\left[(1+\kappa_1)^2 v_{21} + (1+e\kappa_2)\left(e(1+\kappa_2)+2(1-e)\right)v_{22} - (1+\kappa_1)\left(e(1+\kappa_2)v_{23} + (1-e)\right)v_{24}\right],$$

$$u_{21}(p) = \sin^2\alpha - \sin^2 p(\pi-\alpha), \qquad u_{22}(p) = 4p(p-1)\sin^2\alpha\cos^2 p\alpha + u_{21}(p),$$

$$u_{23}(p) = 2(p-1)\sin^2\alpha\cos^2 p\alpha + u_{21}(p),$$

$$v_{21}(p) = (p\cos^2 p\alpha + \sin^2 p\alpha)\sin^2\alpha - \sin^2 p(\pi-\alpha),$$

$$v_{22}(p) = p(p-1)\sin^2\alpha \sin p(\pi-2\alpha)\sin p\pi,$$

$$v_{23}(p) = v_{21}(p) + v_{22}(p) + 2p(p-1)\sin^2\alpha\cos^2 p\alpha,$$

$$v_{24}(p) = p^2\sin^2\alpha\left(\cos 2p\alpha + \sin^2 p(\pi-\alpha)\right) + \sin^2\alpha\sin^2 p\alpha$$

$$-p\sin^2\alpha \sin p\pi\sin p(\pi-2\alpha) - \sin^2 p(\pi-\alpha),$$

where λ_i are the roots of the equation

$$D_1(-1-x) = 0, \tag{14}$$

which meets condition $\operatorname{Re}\lambda_i > -1$.

At the first stage of the development of the plastic zone, when the destruction area is yet absent, the crack opening development at its tip according to boundary conditions $\langle u_\theta(r, \pm\pi)\rangle = 0, \langle u_\theta(r, \alpha)\rangle = 0$ appearing in (1) is equal to zero. For this reason, in accordance with the deformation fracture criterion, the origin of the plastic zone does not influence directly on the crack starting.

2. Determining Parameters of Destruction Area. As it follows from the numerical calculations, equation (14) has roots on the interval $-1 < \operatorname{Re} x < 0$. This indicates that the stress concentration at the crack tip is kept. The experimental studies [17, 24, 25] make it possible to assume the following propagation of the plastic zone by the way of formation within it the area of material destruction with high level both shear and tearing strains. In accordance with the complex model of the interfacial crack [19, 23], we will model the destruction area by the line of length d. On this line, the tangential and normal displacements experience discontinuity, while the normal stress is equal to tearing one σ_1.

With [17, 24, 25], we can assume that the length of the destruction area is much smaller than the length of the plastic zone whole. This makes it possible to consider the body being studied as the piece-wise homogeneous plane with a semi-infinite interfacial crack with faces contacting by the law of dry friction. From the crack tip O a semi-infinite straight discontinuation line issues out at an angle of α to the interface. The line consists of two sections (Fig. 2). On the section OO'' adjacent to the crack tip, the tangential and normal displacements experience discontinuity, while the tangential and normal stresses are equal to τ_1 and σ_1, respectively. On the other section, only the tangential displacement experiences discontinuity, while the tangential stress is equal to τ_1. The present model is consistent with the static elasticity problem with boundary conditions

$$\theta = 0, \qquad \langle\sigma_\theta\rangle = \langle\tau_{r\theta}\rangle = 0, \qquad \langle u_\theta\rangle = \langle u_r\rangle = 0,$$

$$\theta = \pm\pi, \qquad \langle\sigma_\theta\rangle = \langle\tau_{r\theta}\rangle = 0, \qquad \langle u_\theta\rangle = 0, \qquad \tau_{r\theta} = -\mu\sigma_\theta,$$

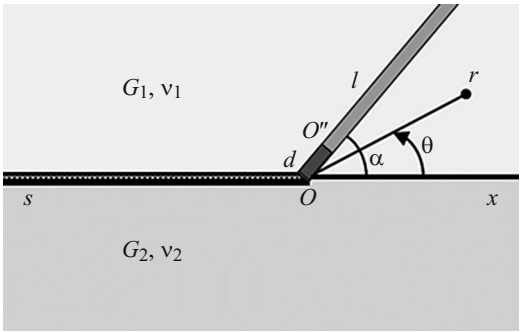


Fig. 2

$$\theta = \alpha, \quad \langle \sigma_\theta \rangle = \langle \tau_{r\theta} \rangle = 0, \quad \theta = \alpha, \quad \tau_{r\theta} = \tau_1, \tag{15}$$

$$\theta = \alpha, \quad r < d, \quad \sigma_\theta = \sigma_1, \quad \theta = \alpha, \quad r > d, \quad \langle u_\theta \rangle = 0. \tag{16}$$

At $r \to \infty$, the main terms of stress expansion into asymptotic series coincide with the main terms of expansions into asymptotic series at $r \to 0$ in the problem shown in Fig. 1. Note that it was solved earlier. So, with (13), we have

$$\theta = \alpha, \quad r \to \infty, \quad \sigma_\theta = f_1(\alpha, e, \nu_1, \nu_2)\tau_1 + \sum_{i=1}^{2} C_i f_{2i}(\alpha, e, \nu_1, \nu_2) r^{\lambda_i} + o(1/r), \tag{17}$$

where $C_i = \tau_1 l^{-\lambda_i}$, l is the length of the whole plastic zone found previously; λ_i are the roots of equation (14) on the interval $-1 < \operatorname{Re} x < 0$. From these roots, two are real:

$$f_1 = \frac{N(-1)}{D_1(-1)}, \quad f_{2i} = \frac{N(-1-\lambda_i)}{D_1'(-1-\lambda_i)} \frac{K^+(-1-\lambda_i)}{K^+(-1)} \frac{J(\lambda_i)}{J(0)} \frac{\lambda}{\lambda_i(\lambda_i - \lambda)}.$$

It is assumed that at the stage of the development of the plastic zone when the destruction area being absent yet, the normal stress near the crack tip at $\theta = \alpha$ is tensile, i.e., $\sigma_\theta > 0$.

At the end O'' of the destruction area, the root singularity holds:

$$\theta = \alpha, \quad r \to d + 0, \quad \sigma_\theta \sim \frac{K}{\sqrt{2\pi(r-d)}}, \tag{18}$$

where K is the stress intensity factor which is determined during the problem solving.

Using the Mellin integral transformation, we reduce the solution of the boundary-value problem (15)–(18) to the functional Wiener–Hopf equation

$$\Phi_1^+(p) + \frac{\sigma_1 - f_1\tau_1}{p+1} - \sum_{i=1}^{2} \frac{C_i f_{2i} d^{\lambda_i}}{p+\lambda_i+1} = -\tan p\pi \cdot H(p)\Phi_1^-(p) \quad (-\varepsilon_1 < \operatorname{Re} p < \varepsilon_2), \tag{19}$$

$$\Phi_1^+(p) = \int_1^\infty \sigma_\theta(\rho d, \alpha)\rho^p d\rho, \quad \Phi_1^-(p) = \frac{G_1}{2(1-\nu_1)} \int_0^1 \left\langle \frac{\partial u_\theta}{\partial r} \right\rangle \Bigg|_{\substack{r=\rho d \\ \theta=\alpha}} \rho^p d\rho,$$

$$H(p) = -\frac{\cos p\pi D_2(p)}{2\sin^2 p\pi D_1(p)}, \quad D_2(p) = D_{20}(p) + 4\mu D_{21}(p),$$

where ε_1 and ε_2 are the sufficiently small positive numbers. The solution of equation (19) obtained in the previous part of the present paper by analogy with the solution of equation (6) has the following form:

$$\Phi_1^+(p) = -\frac{pH^+(p)}{K^+(p)}\left\{\frac{\sigma_1 - f_1\tau_1}{p+1}\left[\frac{K^+(p)}{pH^+(p)} + \frac{K^+(-1)}{H^+(-1)}\right]\right.$$

$$\left. -\sum_{i=1}^{2}\frac{C_i f_{2i} d^{\lambda_i}}{p+1+\lambda_i}\left[\frac{K^+(p)}{pH^+(p)} + \frac{K^+(-1-\lambda_i)}{(1+\lambda_i)H^+(-1-\lambda_i)}\right]\right\} \quad (\mathrm{Re}\, p < 0),$$

$$\Phi_1^-(p) = K^-(p)H^-(p)\left[\frac{(\sigma_1 - f_1\tau_1)K^+(-1)}{(p+1)H^+(-1)}\right.$$

$$\left. -\sum_{i=1}^{2}\frac{C_i f_{2i} d^{\lambda_i} K^+(-1-\lambda_i)}{(p+1+\lambda_i)(1+\lambda_i)H^+(-1-\lambda_i)}\right] \quad (\mathrm{Re}\, p > 0), \tag{20}$$

$$\exp\left[\frac{1}{2\pi i}\int_{-i\infty}^{i\infty}\frac{\ln H(z)}{z-p}\,dz\right] = \begin{cases} H^+(p), & \mathrm{Re}\, p < 0, \\ H^-(p), & \mathrm{Re}\, p > 0. \end{cases}$$

Applying the Abel-type theorem [33] to asymptotic (18), with solution (20), we find by analogy with (10) the stress intensity factor at the end OO'' of the discontinuity line:

$$K = -\sqrt{2d}\left[\frac{(\sigma_1 - f_1\tau_1)K^+(-1)}{H^+(-1)} - \sum_{i=1}^{2}\frac{C_i f_{2i} d^{\lambda_i} K^+(-1-\lambda_i)}{(1+\lambda_i)H^+(-1-\lambda_i)}\right].$$

Equating K to zero, we arrive at the transcendental equation for calculating the length of the destruction area:

$$\sum_{i=1}^{2}\frac{f_{2i}K^+(-1-\lambda_i)J_2(0)}{(1+\lambda_i)K^+(-1)J_2(\lambda_i)}\left(\frac{d}{l}\right)^{\lambda_i} = \frac{\sigma_1}{\tau_1} - f_1, \tag{21}$$

$$J_2(x) = \exp\left[\frac{1}{\pi}\int_0^{\infty}\frac{(x+1)\ln|H(it)| + t\cdot\arg(H(it))}{t^2 + (x+1)^2}\,dt\right].$$

With origin of the destruction area, the SSS near the crack tip changes which is now characterized by the indicator of the stress singularity λ_{d1} which is determined as the root of the equation least from the interval (–1, 0):

$$D_2(-1-x) = 0. \tag{22}$$

If the crack opening displacement at the crack tip as well as the destruction area are absent, the origin of the destruction area leads to the nonzero shear displacement of the faces $\delta = \lim_{x\to -0}|\langle u\rangle_{y=0}|$ at the tip. The displacement due to the jump of the normal displacement $\langle u_\theta(0,\alpha)\rangle$ is related to the expression $\delta = \langle u_\theta(0,\alpha)\rangle / \sin\alpha$. The last one can be defined using its relation with the function $\Phi_1^-(p)$ established in solving the problem

$$\langle u_\theta(0,\alpha)\rangle = -\left\langle\frac{\partial u_\theta}{\partial r}\right\rangle^*\Bigg|_{p=0,\theta=\alpha} = -\frac{2(1-\nu_1)d}{G_1}\Phi_1^-(0).$$

Using (20) and condition $K = 0$, we obtain

$$\delta = -\frac{2(1-\nu_1)\tau_1}{G_1\sin\alpha}\frac{d}{\sqrt{\pi H(0)}}\sum_{i=1}^{2}\frac{f_{2i}K^+(-1-\lambda_i)}{J_2(\lambda_i)}\left(\frac{d}{l}\right)^{\lambda_i}\frac{\lambda_i}{(1+\lambda_i)^2}. \tag{23}$$

The shear of faces δ affects the general crack opening displacement and must be taken in account in studying the conditions at which the crack starts.

3. Numerical Analysis of Parameters of Initial Plastic Zone. As it follows from the previous consideration, the parameters of the small-scale plastic zone and the destruction zone are completely determined by mechanical characteristics of joined materials and the stress intensity factor k_{II}, which can be found separately for the piece-wise homogeneous bodies of corresponding structure as well of the value and kind of external loading either by numerical or analytical solving the boundary-value elasticity problem. Since the last action is not the aim of the present work, to demonstrate the application of the above solution of the problem on the plastic zone and with the aim to analyze its consequences, we will use the results from [33] related to the investigation of a contact zone at the tip of the internal interfacial crack of the length L in the piece-wise homogeneous plane loaded at infinity by a constant tangential force $q(\tau_{xy} \to -q$ at $x^2 + y^2 \to \infty$, Fig. 1).

With the calculations by formula (12), the energy dissipation maximal rate criterion leads to two values of the angle of inclination of an initial plastic zone. One of the angles is blunt and corresponds to the rotation of the zone in the direction of the applied load, while other one is equal to zero and specifies the propagation of the zone along the interface. This agrees with the results of numerical modeling of plastic zones near the tips of interfacial cracks presented in [2, 3, 35] as well as with the presence of two extremums in the angular dependency of the tangential stress (3). Since the problem on the plastic zone along the interface within the framework of the complex model of the interfacial crack has boundary conditions slightly differing from (1)–(4), we will restrict our consideration to the zone with the inclination angle beyond zero. It should be noted that the sufficiently great number of publications (for example, [16, 20, 29]) is devoted to studying the plastic zones on the interface within the framework of various models.

The calculated parameters of the plastic zone (it is the angle of inclination α to the interface between materials, the relative lengths s/L of the contact zone, the lengths l/L and d/L of the whole zone and of the destruction zone) are collected in a Table for some ratios of shear moduli G_1/G_2 of the joined materials with similar Poisson's ratios $\nu_1 = \nu_2 = 0.3$, a number of values of friction coefficients μ, yield points $\tau_{1s} = 0.1G_1$, and external load $q = 0.02G_1$. In calculating the parameters of the destruction area, the rupture strength of the first material was adopted as $\sigma_1 = 2G_1$. The input parameters were chosen in such a way that the conditions $d << l << s$ and $\mu \cot\alpha < 1$, accepted in the model being studied, would be met.

According to the calculations, the length of the whole plastic zone at small ratios of shear moduli G_1 / G_2 in the accepted loading conditions decreases. If the values of G_1 and G_2 are close, it increases with the friction between the crack faces as distinguished from the length of the destruction area, which increases with friction at any values of $G_1 / G_2 < 1$. As it turned out, the length of the plastic zone is two orders of magnitude fewer than that of the contact zone, while the length of the destruction area occurs in turn two order less than the length of the whole zone. Because of this, the application of the above model under sufficiently low loads is fully justified.

At small ratios of G_1 / G_2, the angle of inclination of the plastic zone decreases with increasing the friction, while at close values of G_1 and G_2 it increases. According to (12), the value of the load applied to the piece-wise homogeneous body with the interfacial crack does not affect the orientation of the zone, which by this means depends only on the elastic characteristics of composite materials and the coefficient of friction between the crack faces. Because the angle of inclination of the plastic zone is independent of the external loading, the results obtained differ from the similar study, which has been carried out within the framework of the open interfacial crack model [18]. Besides, the values of the angle of inclination of the zone at the end of the crack calculated in [18] without allowance for the contact of faces under the condition of pure shear are close to those found in the present work.

The table summarizes the values of the singularity level of stresses at the crack tip down to λ once the initial plastic zone λ_1 and the destruction area λ_{d1} have been formed. The comparison λ and λ_1 shows that the origin of the initial plastic zone leads to increase of the stress concentration in the vicinity of the tips $\lambda_1 < \lambda$. As a result, the following propagation of the plastic zone continues with formation of the destruction zone. But this does not remove the stress concentration and causes only its slight decreasing in comparison with the initial level. So, the least root λ_{d1} in (22) from the interval (–1, 0) is slightly larger than the singularity level λ before the formation of both zones $\lambda_{d1} > \lambda$. For this reason the propagation of the plastic zone continues with the formation of new zones, in particular, the above plastic zone along the interface.

Sizes of the area within which the crack faces are in contact under a given type of loading are independent of its modulus [1, 9, 33]. At the same time, the length of the plastic zone increases with the shear stress to the yield point $q > \tau_s$ and approaches (in order of the value) the length of the contact area. In Fig. 3 the solid lines refer to $G_1 / G_2 = 0.1$, dotted ones refer to $G_1/G_2 =$

TABLE

G_1 / G_2	μ	0	–0.1	–0.2	–0.3	–0.4	–0.5
0.1	α, deg	127.4	126.8	126.2	125.8	125.3	125.0
	s / L	0.3098	0.3133	0.3168	0.3203	0.3239	0.3276
	l / L	$8.347 \cdot 10^{-3}$	$7.987 \cdot 10^{-3}$	$7.646 \cdot 10^{-3}$	$7.319 \cdot 10^{-3}$	$7.008 \cdot 10^{-3}$	$6.714 \cdot 10^{-3}$
	d / L	$6.998 \cdot 10^{-5}$	$7.597 \cdot 10^{-5}$	$8.699 \cdot 10^{-5}$	$8.739 \cdot 10^{-5}$	$9.289 \cdot 10^{-5}$	$9.831 \cdot 10^{-5}$
	λ	–0.5	–0.4926	–0.4851	–0.4777	–0.4703	–0.4630
	λ_1	–0.6575	–0.6739	–0.6900	–0.7064	–0.7222	–0.7386
	λ_{d1}	–0.4153	–0.4148	–0.4143	–0.4140	–0.4135	–0.4132
0.9	α, deg	127.8	128.2	128.6	129.1	129.8	130.7
	s / L	0.3052	0.3054	0.3056	0.3059	0.3061	0.3063
	l / L	$6.774 \cdot 10^{-3}$	$6.809 \cdot 10^{-3}$	$6.849 \cdot 10^{-3}$	$6.891 \cdot 10^{-3}$	$6.933 \cdot 10^{-3}$	$6.977 \cdot 10^{-3}$
	d / L	$7.553 \cdot 10^{-5}$	$8.747 \cdot 10^{-5}$	$1.006 \cdot 10^{-4}$	$1.152 \cdot 10^{-4}$	$1.317 \cdot 10^{-4}$	$1.509 \cdot 10^{-4}$
	λ	–0.5	–0.4995	–0.4990	–0.4986	–0.4981	–0.4976
	λ_1	–0.7117	–0.7296	–0.7478	–0.7668	–0.7873	–0.8100
	λ_{d1}	–0.4963	–0.4963	–0.4964	–0.4965	–0.4966	–0.4967

0.9, $\tau_{1s} = 0.1G_1$, $\sigma_1 = 2G_1$, $\mu = -0.2$). In this case the outlet condition of the model concerning the small scale of the zone $l << s$ is disrupted. At the same time, we can see how the plastic and contact zones interact. This can be studied within the framework of the complex model of the interfacial crack in the same way as in [10]. On the contrary, with allowance for the conditions accepted in constructing Fig. 3, the inequality $d << l$ appearing in the model being considered is kept. At that time according to (21), the ratio in sizes of the plastic and destruction zones is independent of the load value if $d / l = 0.0107$ at $G_1 / G_2 = 0.1$ and $d / l = 0.0147$ at $G_1 / G_2 = 0.9$.

Proportions between the sizes of the plastic and destruction zones depend considerably not only on the ratio of shear moduli of joined materials but on the ratio between values of the yield point and rupture stress of the material in which the zones propagate. Figure 4 shows how the value of d / l depends on the rupture stress value at $G_1 / G_2 = 0.1$ (solid lines) and for $G_1 / G_2 = 0.9$ (dotted lines), $\mu = -0.2$ at constant load $q = 0.2\tau_{1s}$. In accordance with Fig. 4, the larger the ratio d / l, the less the rupture stress or the larger the yield point. This can lead to the disruption of the condition $d << l$, which corresponds to the case with the destruction zone being fewer the plastic one. In this case, the material can be considered as quasi-brittle one and the more complex strength criterion should be employed against the above used Tresca–Saint-Venant one-parametric plasticity criterion. As an alternative for the above model, in the case of a quasi-brittle material we can use model [22] of a prefracture zone near the tip of a completely open interfacial crack. The model is based on the employment of the Mises–Hill-type quadratic strength criterion with the yield point and rupture stress as criterion parameters.

As shown in Fig. 3, the d / l ratio for the fixed characteristics of the materials is constant and independent of the acting loads. Because of this, according to (23), the shear displacement δ of the crack faces at its tip is directly proportional to the length

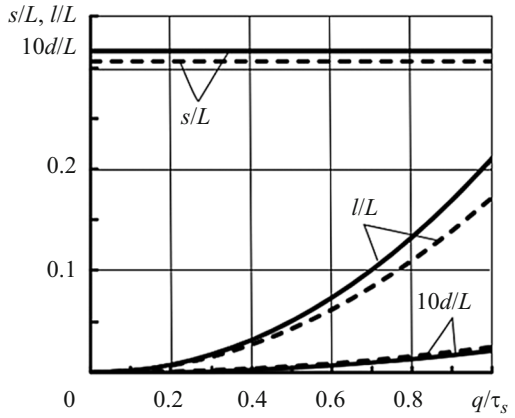


Fig. 3

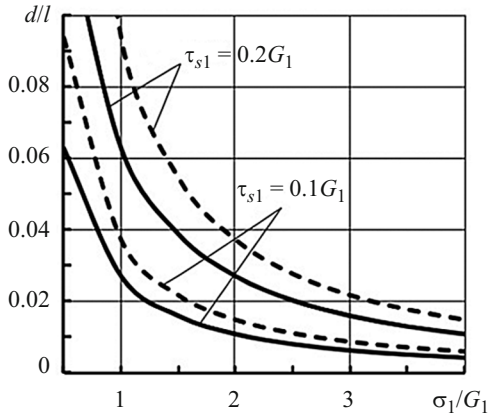


Fig. 4

of the destruction zone and nonlinearly increases with the applied load. This makes it possible to assume that the crack may start due to the breakage of interparticle bonds in the destruction zone and to determine the limiting load by one or other strain criterion.

Conclusions. Within the framework of the complex model of the interfacial crack, we have developed the model of the initial plastic zone under shear. The model describes the mechanism of crack's propagation in an elastoplastic body. Near the crack tip, the faces contact area and narrow plastic zone are formed in one of the composite materials, while the strongly deformed zone of destructed material arises in the section adjacent to the area. Presence of the zones leads to the relative shear of the tips of both crack's faces. The sizes of plastic and destruction zones as well as the shear displacement of the crack faces at the crack's tip increase with the load facilitating that contributes to crack's starting.

REFERENCES

1. Yu. A. Antipov, "An interface crack between elastic materials when there is dry friction," *J. Appl. Math.*, *Mech.*, **59**, No. 2, 273–287 (1995).
2. N. Aravas and S. M. Sharma, "An elastoplastic analysis of the interface crack with contact zones," *J. Mech. Phys. Solids*, **39**, No. 3, 311–344 (1991).
3. N. Aravas and S. M. Sharma, "Plane stress elastoplastic solutions of interface cracks with contact zones," *Mech. Mater.*, **12**, No. 2, 147–163 (1991).
4. C. Atkinson, "The interface crack with a contact zone," *Int. J. Fract.*, **18**, 161–177 (1982).
5. G. P. Cherepanov, "General theory of failure," *Mater Sci.*, **22**, No. 1, 32–39 (1986).
6. G. P. Cherepanov, *Mechanics of Brittle Fracture*, McGraw-Hill, New York (1979).
7. M. Comninou, "Interface crack with friction in the contact zone," *J. Appl. Mech. Trans. ASME*, **44**, No. 4, 780–781 (1977).
8. M. Comninou, "The interface crack," *J. Appl. Mech. Trans. ASME*, **44**, No. 4, 631–636 (1977).
9. M. Comninou and J. Dundurs, "Effect of friction on the interface crack loaded in shear," *J. Elast.*, **10**, 203–212 (1980).
10. M. V. Dudyk, "Mutual influence of the faces contact and the pre-fracture zone near the tip of the interfacial crack," *Strength Fract. Complex.*, **13**, 143–161 (2020).
11. D. Dugdale, "Yielding of steel sheets containing slits," *J. Mech. Phys. Solids*, **8**, No. 2, 100–104 (1960).
12. J. Dundurs, "Discussion: "Edge-bonded dissimilar orthogonal elastic wedges under normal and shear loading," *J. Appl. Mech. Trans. ASME*, **36**, No. 3, 650–652 (1969).
13. F. D. Gakhov, *Boundary Value Problems*, Pergamon Press, Oxford (1966).
14. A. K. Gautesen and J. Dundurs, "The interface crack under combined loading," *J. Appl. Mech. Trans. ASME*, **55**, No. 3, 580–586 (1988).

15. K. P. Herrmann and V. V. Loboda, “On interface crack models with contact zones situated in an anisotropic bimaterial,” *Arch. Appl. Mech.*, **69**, 311–335 (1999).
16. A. A. Kaminskii, L. A. Kipnis, and V.A. Kolmakova, “Slip lines at the end of a cut at the interface of different media,” *Int. Appl. Mech.*, **31**, No. 6, 491–495 (1995).
17. A. A. Kaminskii, G. I. Usikova and E. A. Dmitrieva, “Experimental study of the distribution of plastic strains near a crack tip during static loading,” *Int. Appl. Mech.*, **30**, No. 11, 892–897 (1994).
18. A. A. Kaminsky, M. V. Dudyk, and L. A. Kipnis, “On the direction of development of a thin prefracture process zone at the tip of an interfacial crack between dissimilar media,” *Int. Appl. Mech.*, **42**, No. 2, 136–144 (2006).
19. A. O. Kaminsky and M. V. Dudyk, “Analytical methods of modeling the prefracture zone near an interfacial crack tip (Review),” *Int. Appl. Mech.*, **59**, No. 5, 505–539 (2023).
20. A. O. Kaminsky, M. V. Dudyk, and V. M. Fenkiv, “Starting of an interfacial crack with contacting faces from the corner point of a polygonal interface,” *Int. Appl. Mech.*, **58**, No. 5, 533–544 (2022).
21. A. O. Kaminsky, M. V. Dudyk, V.M. Fenkiv, and Y. O. Chornoivan, “On the scope and limitations of the Comninou model for a crack at a polygonal interface,” *Int. Appl. Mech.*, **58**, No. 4, 398–409 (2022).
22. A. O. Kaminsky, M. V. Dudyk, Y. V.Reshitnyk, and Y.O. Chornoivan, “An analytical method of modeling the process zone near the tip of an interface crack due to its kinking from the interface of quasi-elastic materials,” *Int. J. Solids Struct.*, **267**, No. 112117 (2023).
23. A. O. Kamins’kyi, M. V. Dudyk, and L. A. Kipnis, “Investigation of the process zone near the tip of an interface crack in an elastic body in shear within the framework of the complex model,” *J. Math. Sci.*, **220**, No. 2, 117–132 (2017).
24. I. S. Kohut and H. I. Kalyta, “Evaluation of the sizes of the process zone for quasibrittle notched specimens,” *Mater. Sci.*, **44**, No. 1, 97–103 (2008).
25. E. E. Kurchakov, “Experimental study of the plastic zone at the front of a mode I crack,” *Int. Appl. Mech.*, **54**, No. 2, 213–219 (2018).
26. J. B. Leblond and J. Frelat, “Crack kinking from an initially closed, ordinary on interface crack, in the presence of friction,” *Eng. Fract. Mech.*, **71**, No. 3, 289–307 (2004).
27. M. Y. Leonov and V. V. Panasyuk, “Growth of the smallest cracks in solids,” *Prikladna Mech*. (*Appl. Mech.*) [in Russian], **5**, No. 4, 391–401 (1959).
28. V. V. Loboda, “Analytical derivation and investigation of the interface crack models,” *Int. J. Solids Struct.*, **35**, No. 33, 4477–4489 (1998).
29. V. V. Loboda and A. E. Sheveleva, “Determining prefracture zones at a crack tip between two elastic orthotropic bodies,” *Int. Appl. Mech.*, **39**, No. 5, 566–572 (2003).
30. A. Nakatani, W. J. Drugan, E. Van der Gissen, and A. Needleman, “Crack tip fields at a ductile single crystal-rigid material interface,” *Int. J. Fract.*, **122**, 131–159 (2003).
31. A. H. Nayfeh, *Perturbation Methods*, Wiley-Interscience, New York (1973).
32. B. Noble, *Methods based on the Wiener-Hoph Technique* for the Solution of Partial Differential Equations. 2nd ed., Chelsea Pub. Co., New York (1988).
33. V. I. Ostrik, “Friction contact of the edges of an interface crack under the conditions of tension and shear,” *Mater. Sci.*, **39**, No. 2, 214–224 (2003).
34. V. V. Panasyuk and M. P. Savruk, “Model for plasticity bands in elastoplastic failure mechanics,” *Mater. Sci.*, **28**, No. 1, 41–57 (1992).
35. C. F. Shih and R. J. Asaro, “Elasto-plastic analysis of cracks on bimaterial interfaces: Part II - Structure of small-scale yielding fields,” *J. Appl. Mech.*, **56**, No. 4, 763–779 (1989).
36. Ya. S. Uflyand, *Survey of Articles on the Application of Integral Transforms in the Theory of Elasticity*, North Carolina State University, Raleigh (1965).